Received: 7 December 2022 | Revised: 25 February 2023 | Accepted: 13 March 2023

DOI: 10.1002/pc.27324

RESEARCH ARTICLE

Polymer COMPOSITES WILEY

Characterization of moisture absorption and flexural performance of functionalized graphene modified carbon fiber composites under low energy impact

Feras Korkees[1] | **Elliot Morris**[1] | **William Jarrett**[2] | **Russo Swart**[1]

[1]Department of Materials Science and Engineering, Faculty of Science and Engineering, Bay Campus, Swansea University, Swansea SA1 8EN, UK

[2]Institute of Structural Materials, Faculty of Science and Engineering, Bay Campus, Swansea University, Swansea SA1 8EN, UK

Correspondence
Feras Korkees, Department of Materials Science and Engineering, Faculty of Science and Engineering, Bay Campus, Swansea University, Swansea, SA1 8EN, UK.
Email: f.a.korkees@swansea.ac.uk

Abstract

Composite failure due to in-service low energy impact damage and moisture absorption is a major risk for these materials within aerospace, automotive and other engineering sectors. Deterioration in post-impact flexural properties, and the tendency of thermosets to absorb moisture are some of the few drawbacks of carbon fiber reinforced polymers (CFRPs). Adding graphene into the matrix is theorized to improve mechanical properties and reduce moisture uptake. This study evaluates the diffusion characteristics and flexural properties of carbon fiber/epoxy composites modified with NH_2 functionalized graphene (CFRP/graphene nanoparticle [GNPs]) before and after impact under various environmental conditions. Adding GNPs to CFRP decreased the flexural strength and modulus by 24% and 25% respectively before impact. After impact, the flexural strength and modulus decreased by 7.4%–23.6% and 37%–67%, respectively. For both composites after undergoing impact, the residual strength and stiffness were considerably reduced due to delamination and transverse cracking. Samples with graphene inclusion experienced a slower rate of ethanol and water diffusion, for both unimpacted and impacted samples, by 46.4% and 44.8%, respectively. Moisture uptake also reduced the flexural properties of both composites. Scanning electron microscopy revealed good dispersion but poor bonding of graphene to the matrix, which is believed to be the reason for property reduction.

KEYWORDS

carbon fibers, drop-weight testing, flexural properties, graphene nanocomposites, moisture diffusion

1 | INTRODUCTION

The use of composites has become integral to the aerospace, automotive, sports, and defense industry. Apart from increased strength at lower weights, composites also meet fatigue, damage tolerance, corrosion resistance, gust alleviation, and low noise footprint requirements.[1] For instance, the Airbus A350XWB consists of 53% composite material, reducing the aircraft weight and increasing the service intervals for the aircraft from

6 to 12 years, significantly reducing maintenance costs for the customers.[2,3]

The limitations of carbon fiber reinforced polymer (CFRP), however, are their susceptibility to impact damage, which in general limits their practicality for such applications; once impacted, the residual properties of CFRP change considerably. During the service life of composites, accidental impact damage at a high strain rate during routine maintenance, hail, debris strike on the runway or during flight is a major concern, as it leads to catastrophic failure, resulting in complex fracture mechanisms and damage that is usually microscopic and invisible to the naked eye.[4,5] This normally leads to reductions in stiffness and strength, especially under hot/wet environments.[6] Several studies[4,6–11] reported a 30%–50% reduction in the strength of composite materials after a low-energy impact. This reduction was found to be a result of intra-matrix cracking, delamination, and de-bonding between fibers and the matrix. Furthermore, the exposure of composite materials to hot/wet environments normally leads to plasticization, hydrolysis, interface debonding, and micro-cracking. There have been many studies[12–26] that investigated the moisture absorption behavior and hygrothermal effects on the mechanical properties of polymer composite materials. These hygrothermal effects and low energy impact damage can affect the overall performance of CFRP such as stiffness and strength.[17,25–27] Therefore, improvements to the toughness characteristics and reduction in moisture absorption of composites are seen as desirable.

Nanoscale reinforcement is a rapidly growing interest within the materials industry, as they offer the possibility of improving the mechanical and physical performance of composites, including compression and interlaminar properties.[28] Graphene is the first two-dimensional atomic crystal, and in recent years there has been a significant advancement in the mass production of this material. Graphene combines strong mechanical properties with exceptionally high electric and thermal conductivity properties.[29,30] This material also has significant gas and moisture barrier properties.[31] However, the cost of graphene nanoparticles, their availability and the challenge to achieve good dispersion pose significant obstacles to achieving these goals.[32] Nanoparticle-reinforced polymer composites have now attracted more attention in various engineering applications. The high specific surface area of nanoparticles allows the formation of a strong interaction between the fillers and the matrix. Therefore, the unique properties of nanocomposites result from nano-scale structures.[33] The nanomaterials used to enhance the various properties of the bulk composite materials include graphene, carbon black, ZnO_2, Fe_2O_3, nanoclays, carbon nanotubes (CNT, SWCNT, MWCNT), $CaCO_3$, rubber, and nanocellulose.[34] The flexural and impact properties of carbon fiber reinforced epoxy composites modified with 2 wt% montmorillonite nanoclay and 0.3 wt% multi-walled carbon nanotubes (MWCNTs) were studied by[35] and a significant improvement in properties was observed by the addition of nanoparticles. The addition of graphene to carbon fiber composite have been reported to improve the water uptake resistance by 43.9% but reduced the interlaminar shear strength after immersion in water by an average of 5.8%.[36] The effects of adding reinforcing nanoparticles on the fatigue and tensile properties of polymer composite was studied by Knoll et al.[37] and Abu-Okail et al.[38] and improvements in both properties were observed. It was also reported that the addition of other nanoparticles into CFRP increased the composite strength and enhanced the weathering stability depending on the nanoparticles used.[39] Moreover, an improvement in the tensile strength, stiffness and impact properties was reported by Sivasaravanan et al.[40] and Gabr et al.[41] with the addition of 3 wt% nanoclay to carbon fiber composites. Koricho et al.[42] investigated the effect of hybrid (micro- and nano-) fillers on the impact response of glass fiber reinforced plastic composite. Their results showed better damage distribution with nanofillers, which improved the resistance to delamination and intralaminar crack formation. On the contrary, a reduction in the tensile and flexural behavior of carbon fiber/epoxy laminates was reported by Watson et al.[43] with the addition of graphene oxide which was caused by agglomeration, poor dispersion and bonding difficulty. Furthermore, a study conducted by Zhao et al.[44] concluded that the flexural strength and modulus of the CF/epoxy composites initially increased, and then decreased with increasing CNT content in the matrix. The influence of nanoparticle agglomeration on the interfacial and tensile properties of nanocomposites was studied by Zare et al.[45] They reported interfacial declination due to agglomeration and poor interfacial strength, which reduced the tensile strength. It is believed, however, that good bonding, compatibility, appropriate loadings, and relatively small-size nanomaterials can reduce the damage initiation of fiber-reinforced polymer composite materials unless either poor dispersion arises, or large concentrations of nanomaterials are formed.[34] Furthermore, moisture absorption in composites reinforced with functionalized graphene oxide nanoparticles was studied by Starkova et al.[46] and lower water diffusivity of 40% was obtained. Another research study by Prolongo et al.[47] showed that the use of graphene reduced the moisture content in epoxy resins.

The functionalization or surface modification of graphene is crucial as it enables it to form stable dispersion

and improve bonding and interaction with the host matrix. The application of using functionalized graphene to improve dispersion and bonding with the epoxy resin in epoxy matrix composites has been theorized to improve the strength and toughness and to reduce moisture absorption.[48,49] Functionalized graphene nanoparticles can act as a load bearer, while also providing obstacles for dislocations and crack propagation. Nanoparticles can effectively suppress the formation and propagation of micro-cracks in the matrix.[50] The detaching between nanoparticles and matrix will create a considerable number of voids,[50] resulting in a larger fracture surface area, which consumes substantial deformation energy. This method has proven successful in drastically improving the strength, interlaminar shear strength (ILSS), energy absorption, and toughness of CFRP.[36,48] Other nanocomposites have also seen improvements in these areas, such as functionalized graphene/nylon composites,[51] SWNT/polymer nanocomposites,[52] and phenylethynyl-terminated polyimide composites.[53] There is still, however, a gap in research and an opportunity to compare the residual flexural properties of carbon fiber composite with and without GNPs at various impact energies and environmental conditions.

This study investigated the effect of the addition of 2 wt% NH_2 functionalized graphene nanoparticles on the impact properties and the residual flexural properties of carbon fiber/epoxy composites (CFRP). A drop-weight impact test was used to impact the composites at low impact energies followed by a 3-point bend testing to evaluate post-impact properties. The hypothesis is that through the process of functionalization, the GNPs are evenly dispersed throughout the matrix with strong bonding so they can act as a load bearer providing obstacles for crack propagation, and hence slow the rate of damage and enhance flexural properties. Water and ethanol absorption was carried out at room temperature to study the diffusion behavior and the effect of GNPs on it. GNPs are believed to further hinder the path of the liquid molecules and slow down the diffusion in CFRP. The effect of moisture absorption on the flexural properties before and after impact was also evaluated. Additionally, the composites were subjected to post-curing and its impact on flexural and diffusion properties was investigated. Optical microscopy was used to determine the failure modes after impact and flexural testing. The dispersion and bonding of GNPs were characterized using scanning electron microscopy (SEM).

2 | MATERIALS AND TESTING

The material used in this study is 2 × 2 twill carbon fiber woven fabric/epoxy composite reinforced with 2 wt% NH_2-GNPs. The 2 × 2 twill carbon fiber woven fabric has a 0.28 mm thickness and orientation [0°, 90°], with each fiber having a 7 μm filament diameter, and tensile strength of 4120 MPa. An IN2 epoxy-infused resin with a tensile strength between 63.5 and 73.5 MPa and T_g onset between 92 and 98°C was used. Both fibers and epoxy were supplied by easy composites. The nanoparticles used were amine functionalized graphene nanoparticles with a specific surface area of 500 m^2/g provided by Perpetuus Carbon Technologies Ltd. Amine-GNPs contained the amine functional group, consisting of basic nitrogen atoms, resulting in hydrogen bonding with other hydroxyl groups, hydrogen atoms and molecules. They were prepared using plasma processing in a multi-electrode dielectric barrier discharge plasma reactor.[36] Here, the graphite powders were exposed to an argon plasma for 60 min at 3 and 6 kW. This exfoliated the graphite and negated the van der Waals forces between the layers. Amine plasma was then used to introduce NH_2 functional groups to reduce the occurrence of agglomeration. The 2 wt% amine GNPs were first mixed with epoxy using shear mixing and a three-roll mills mixer. The composite panels were then manufactured by resin infusion molding. The sheets were cured first at room temperature using UV lights for 24 h followed by 6 h of curing in an oven at 60°C. Samples were cut using a waterjet from the 1 m^2 sheets down to 80 mm × 20 mm sized samples with a thickness of 2 mm.

Impact testing was performed using a drop-weight impact testing rig with a hemispherical nose of 12.7 mm similar to the one used in Korkees et al.[17] The impact rig had a maximum height of 1.2 m. During impact testing, different loads were used to produce different low-impact energies. For each energy produced, 15 samples of CFRP and 15 samples of CFRP with GNPS were tested. Impact energies of 5 and 10 J were decided upon as they would provide the optimum damage to the sample for analysis without excessively damaging the samples, risking shattering. To calculate these impact energies, the following Equation (1) was used[17]:

$$E = h \cdot g \cdot \left(M_h + \frac{W}{g} \right) \quad (1)$$

Where h is the distance from the tip of the hanger to the top of the sample (0.69 m), E is the impact energy required, M_h is the mass of the hanger, and W is the weight placed on top of the hanger. This equation was used to calculate the final impact energies used for impact testing using weights of 5 and 10 N. The final calculated impact energies that have been used throughout the impact testing process are 5 and 10 J.

For the immersion test, the specimens were initially weighed and then fully immersed in water and ethanol at room temperature. The percentage of moisture weight gain versus time was monitored by gravimetric methods for all specimens until the specimens approached effective moisture equilibrium. The specimens used for moisture absorption measurements are the same size as the impact samples. Two to three specimens of each material type were conditioned to get an average of the results. An analytical balance having a precision of 0.1 mg was used to measure the weights of the samples. Liquid uptake was calculated as weight gains related to the weights of the dry samples. The weight gain was calculated using Equation (2):

$$\text{Weight gain } (M_t)\% = \frac{W_t - W_0}{W_0} \times 100 \tag{2}$$

where W_0 is the original dry weight and W_t is the weight after immersion at time t.

Diffusion properties were characterized using maximum liquid content and diffusion coefficients. Some samples did not reach saturation and would have continued to absorb liquids if the experimental time were lengthened. Since the Fickian diffusion model is used, it is necessary to extract the Fickian component of the measured data. Using the derived saturation values (M_∞%), the apparent diffusion coefficients with no edge effects considered were determined using Equation (3).[17,18,26]

$$D_{\text{app}} = \frac{\pi \cdot G^2 \cdot h^2}{16 \cdot M_\infty^2} \tag{3}$$

Where h is the thickness of the sample and G is the gradient determined using Equation (4). It is important to note that the apparent diffusivity is associated only with the initial part of the diffusion curve which is Fickian diffusion.

$$G = \left(\frac{(M_{t2} - M_{t1})}{(\sqrt{t_2} - \sqrt{t_1})}\right) \tag{4}$$

The apparent diffusion coefficient is a one-dimensional approximation and does not consider diffusion through the edges of the specimen. Therefore, a correction derived by Shen and Springer[54] was used to account for the edge effects on diffusion. The corrected diffusion coefficient, D, was calculated using Equation (5) where l is the length, b is the width, and h is the thickness of the samples.[17,18,26]

$$D_{\text{corrected}} = \left(1 + \frac{h}{l} + \frac{h}{b}\right)^2 \times D_{\text{app}} \tag{5}$$

Three-point bend testing following ISO 178 was completed on all samples to determine the flexural properties of the materials. The tests were conducted to evaluate the residual flexural strength of the samples before and after being subjected to moisture absorption and impact. The three-point bending load was applied at a constant crosshead rate of 10 mm min^{-1} on the impacted side of the specimens and perpendicularly to the fibers.

A Keyence VHX-1000 (high depth of field) microscope was used to analyze the structure of samples before and after impact. Samples impacted at 5 and 10 J were investigated to assess the failure modes of samples and the size of impact areas. Unimpacted samples of both CFRP and graphene toughened were also analyzed allowing for a comparison between impacted and as-received samples. An ultra-high resolution analytical JEOL JSM 7800 SEM was also utilized to investigate the dispersion and bonding of graphene nanoparticles within CFRP.

3 | RESULTS AND DISCUSSION

3.1 | Water and ethanol uptake

As can be seen in Figures 1 and 2, standard Fickian diffusion does not seem to have been followed for the uptake of water, however, an interesting three-stage diffusion mechanism was detected for water and ethanol. All samples displayed an initial quick diffusion rate but then followed a slower increase in the water uptake in the second stage before leveling out in the third stage, potentially indicating saturation. The three stages were noted within the same time phase, indicating that this behavior might be due to the characteristics of the epoxy resin including swelling, the high polarity of the polymer, insufficient curing, and high free volume, therefore not be related to the specific diffusion mechanism of these liquids. The actual diffusion behavior of many polymers derives from the concentration-dependent forms of Fick's law with constant boundary conditions, particularly when an extensive swelling of the polymer results from the penetrant diffusion. Normally, this deviation may arise from the structural changes of the polymer due to diffusional mobility.[19] Swelling normally leads to microcrack formation and capillary flow in which liquid ingresses through the pores and microcracks in the bulk resin. A two-stage absorption behavior was reported by many researchers which was attributed to the polymer relaxation phenomenon.[16–22,36]

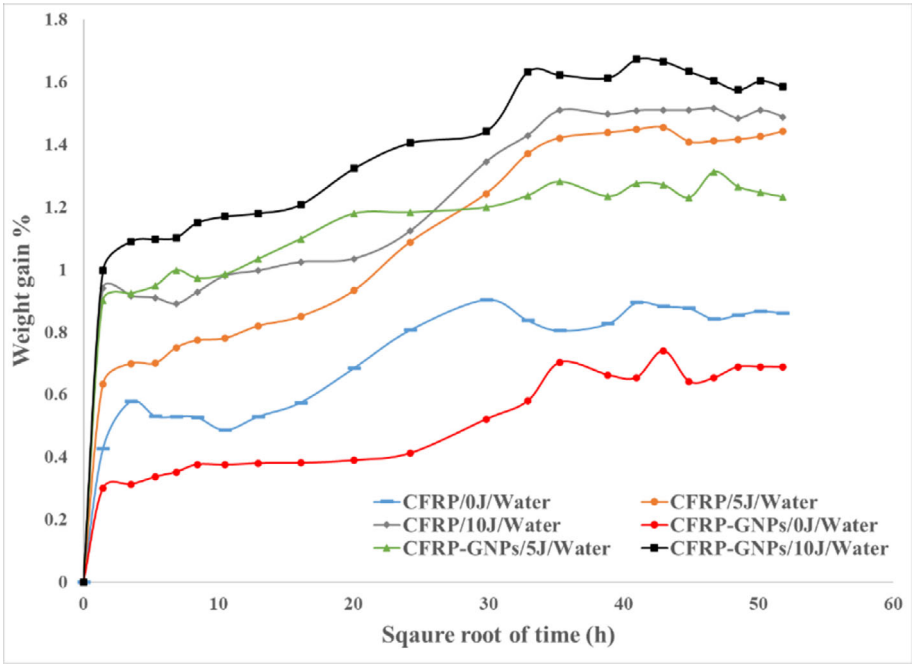

FIGURE 1 Water uptake of carbon fiber reinforced polymer (CFRP) and CFRP/graphene nanoparticles (GNPs) composite samples at all impact energies.

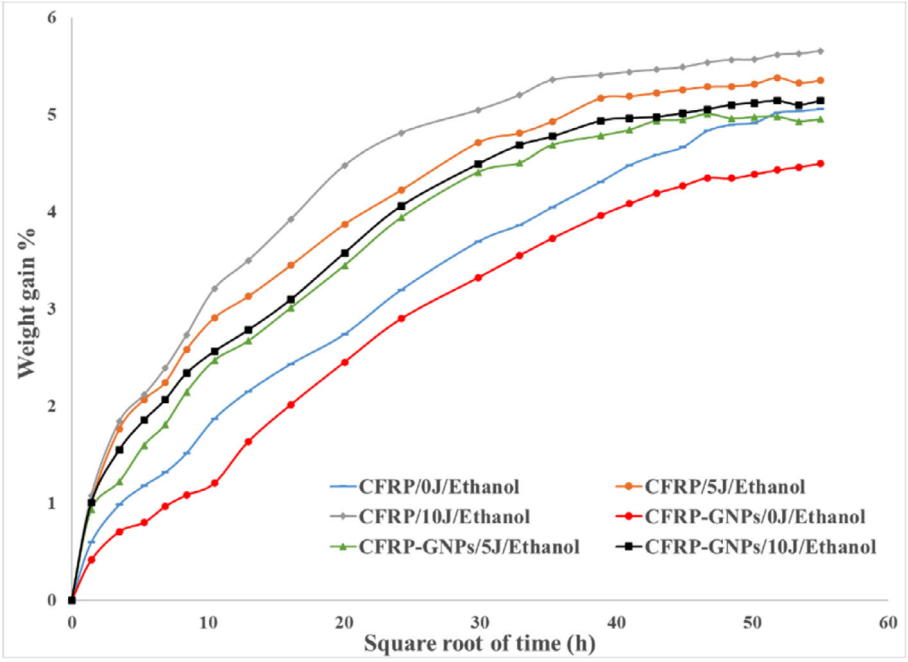

FIGURE 2 Ethanol uptake of carbon fiber reinforced polymer (CFRP) and CFRP/graphene nanoparticles (GNPs) composites at all impact energies.

It also shows that as impacted energy increased, water uptake also increased. This was seen in both CFRP and CFRP/GNPs samples at all energy levels tested. The increased water uptake at higher impact energies may have been induced by an increase in inter-laminar crack formation, matrix cracking, fiber breakage, and chipping of the surface in the material as impact energy increased. The more inter-laminar cracks in the material, the easier it is for water molecules to enter the material, as reported by Korkees et al.[17] Figures 1 and 2 provides evidence of graphene acting as a barrier to moisture absorption in the composite by creating more complicated pathways for water molecules to follow. For unimpacted samples that were immersed in water, the mass gain of CFRP/GNPs is 0.6% compared to 0.8% for CFRPs which is a reduction of 0.2%. This reduction can be attributed to the 'tortuous path' provided by the network of GNPs, which hinders the diffusion of liquid molecules through the matrix.[36]

Ethanol absorption for all samples, Figure 2, displayed much higher mass gain percentages compared to samples that were immersed in water. The higher mass gain is most likely because both ethanol and the epoxy

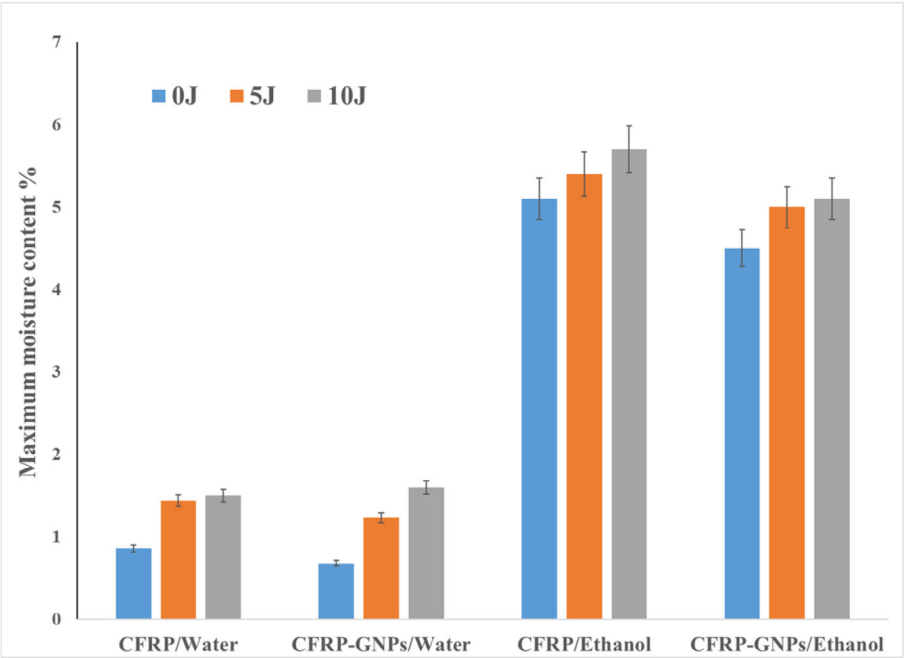

FIGURE 3 Maximum water and ethanol content in carbon fiber reinforced polymer (CFRP) and CFRP/graphene nanoparticles (GNPs) composites at all impact energies.

have OH groups that the epoxy can form bonds or strong polar attraction with the hydroxyl groups. This may have triggered more absorption in the composite. As the epoxy was cured at a low temperature of 60°C, it is possible that a large number of OH groups were available to attract ethanol in the resin bulk.[19] Additionally, swelling could have created a large number of micro-cracks in the interlaminar matrix, resulting in the larger ethanol molecules entering at a greater quantity, displaying a significant amount of mass gain for these samples.

Figure 2 shows that as energy levels increased, percentage mass gain also increased for all samples immersed in ethanol. This appears to be the same as in water-immersed samples. With higher impact energies and increased impact-induced damages (interlaminar crack formation, matrix cracking, fiber breakage, and chipping of the surface), it was made easier for ethanol molecules to enter the material. It provides further evidence that the graphene within the CFRP is an effective method of reducing the absorption of liquids in impacted samples. For ethanol uptake, CFRP/GNPs samples gained (4.5%) on average, which was 0.5% less mass compared to 5% for CFRP samples. This greater reduction in percentage mass could be attributed to the difficult paths for the molecules to navigate past the graphene.[36] For the impacted samples immersed in water and ethanol, there was an increase in the percentage of mass gain to around 1.2%–1.6% and 5%–6%, respectively which indicate that at these impact energies, the damage to the composite is too great for graphene to have any impact on the uptake of water.

3.2 | Diffusion properties

Figure 3 shows that across all samples, as impact energy increased, the maximum moisture content also increased. Furthermore, samples that were immersed in ethanol had a far higher moisture content for all samples.

Both Figures 4 and 5 show that as impact energy increased, the diffusion rate also increased. The ethanol samples in Figure 4 had a higher diffusion rate for all samples and showed a much greater increase in diffusion coefficients after being impacted compared to the water-immersed samples in Figure 5. CFRP/GNPs often had an equal or sometimes lower rate of diffusion for samples that were unimpacted or impacted at 5 J, but at 10 J CFRP samples had a significantly lower diffusion coefficient. The rate of diffusion increased with increasing impact energy which has been replicated in other research[17,55] and is caused by an increase in cracks found at higher impact energies. The higher initial rate of diffusion for ethanol samples compared to water-immersed samples also provides further evidence that there were many OH groups ready to react, which could be a factor in the high percentage mass gain in ethanol-immersed samples. The swelling and degradation of the polymer increased the size and number of micro-cracks, allowing the uptake of higher volumes of ethanol molecules.

Based on the evidence found in Figures 4 and 5, graphene significantly decreased the rate of diffusion for all impact energies. For example, the largest protective decrease in diffusion occurred at 5 J for ethanol, and 10 J

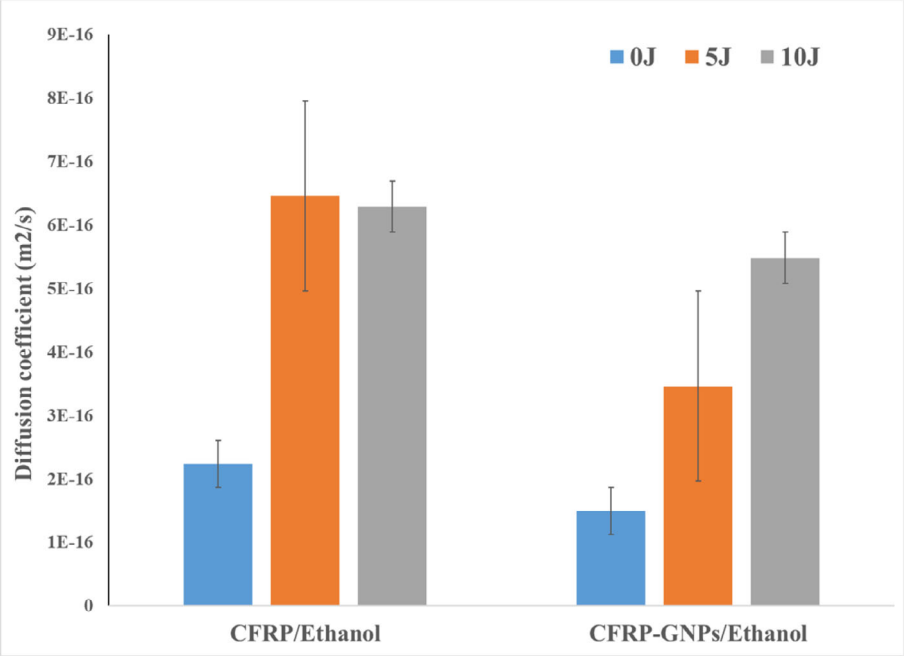

FIGURE 4 Diffusion coefficient of ethanol in carbon fiber reinforced polymer (CFRP) and CFRP/graphene nanoparticles (GNPs) composites at all impact energies.

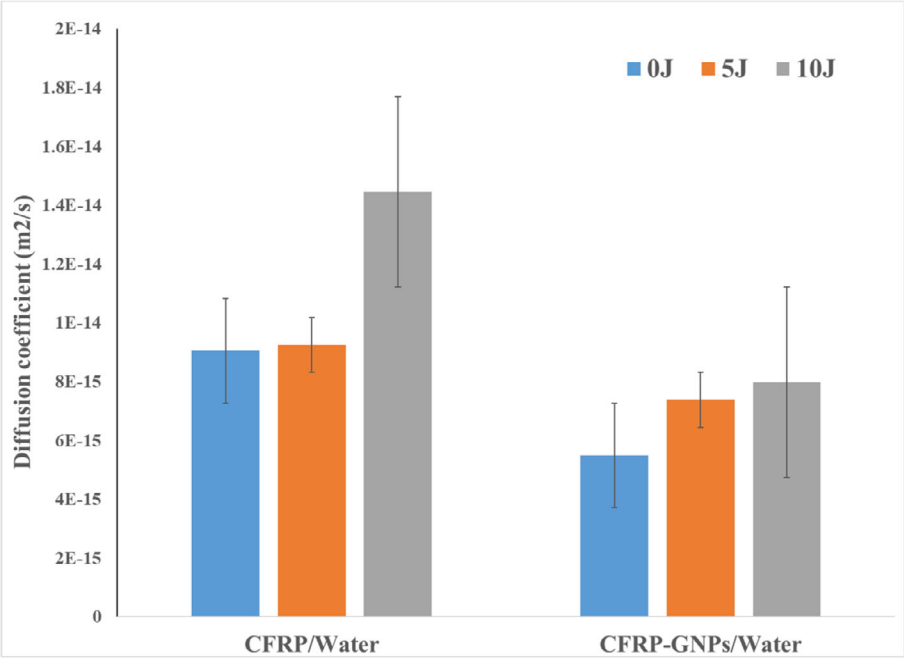

FIGURE 5 Diffusion coefficient of water in carbon fiber reinforced polymer (CFRP) and CFRP/graphene nanoparticles (GNPs) composites at all impact energies.

for water, at 46.4% and 44.8% respectively. For 10 J ethanol exposure, the size and number of cracks could be too large for graphene to have any reasonable effect on the overall diffusion process.

3.3 | Flexural modulus

The average flexural modulus changes across all impact energies and immersion types are highlighted in Figure 6. Five samples at each energy were tested to calculate an average. Flexural modulus was calculated using only the initial gradient of the plots between strain values of 0.0005 and 0.0025. Figure 6 shows that the flexural modulus of the dry and un-impacted CFRP/GNPs samples is 9 GPa lower than that of the CFRP. This means that the addition of NH_2 functionalized graphene reduced the flexural modulus of the composites by 25%. A similar behavior was observed for the unimpacted composites after immersion in water and ethanol but with a larger reduction in flexural modulus of CFRP/GNPs by 45% and 81% respectively compared to

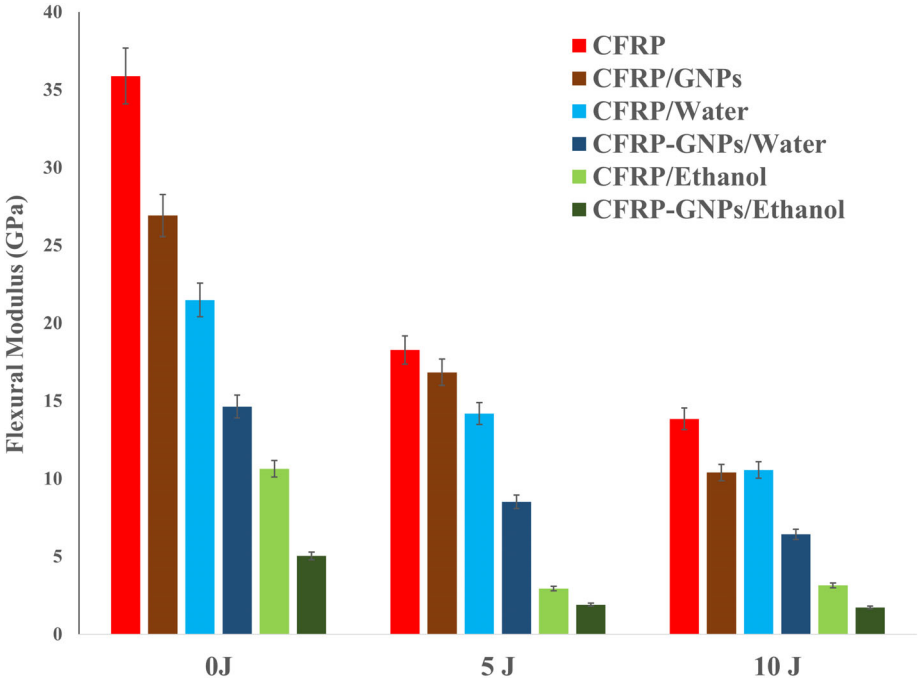

FIGURE 6 Flexural modulus of all samples before and after impact and immersion.

unimpacted and dry CFRP/GNPs. On the other hand, the flexural modulus of CFRP composite decreased by 40% and 70% due to water and ethanol absorption respectively. This highlights the much-reduced qualities of unimpacted CFRP/GNPs compared to CFRP stating that even after immersion in water and ethanol, the unimpacted CFRP composite is still stiffer than the unimpacted CFRP/GNPs composite.

Once impacted, there was a large decrease in the overall stiffness of the composites before and after immersion. This has been evident in several studies previously.[17,29] Interestingly, the results showed that after 5 J impact, the stiffness was reduced by 49% for the CFRP composite while a lower reduction of 37% was observed for the CFRP/GNPs composites. Moreover, a reduction of 61% was observed at 10 J impact for both composites. This suggests that graphene nanoparticles increased the toughness and energy absorption of CF composites by reducing the number of cracks and their propagation in the material.[36,56] Despite that, the data in Figure 6 suggests that the predicted stiffness increase in CFRP/GNPs has not been found, and based on the evidence presented, graphene lowered the flexural modulus of the composite before and after impact and immersion. The main factors that could have contributed to this reduction in the properties are the poor dispersion of graphene due to agglomeration within the composite and poor bonding of graphene with the epoxy in the composite which has been seen to be a common concern with the use of graphene in composites in other studies.[32,36,43–45,51]

Figure 6 shows that at all impact energies, the flexural modulus of both CFRP and CFRP/GNPs decreased by (33%–56%) and (62%–72%) after immersion in water and ethanol for around 2500 h, respectively. This reduction in the flexural properties of the material is caused by liquid molecules diffusing in the bulk of the polymers and the material through the microcracks and voids in the surface of the epoxy. Absorbed liquid molecules can plasticize the polymer and produce damage within the composite mainly in the form of interfacial fiber/matrix microcracks/debonding leading to damaging the interior of the sample.[57] The greater the impact energy, the larger the cracks, and the more water molecules are expected to enter the material. This causes a greater increase in microcracks; therefore, it was expected that greater impact energies would give much lower flexural properties when compared to similarly conditioned as received samples. Figure 6 also shows that water and ethanol-saturated CFRP/GNPs had a significantly further decrease in flexural strength once impacted compared to water and ethanol-saturated CFRP. Furthermore, the further reduction in modulus of samples immersed in ethanol compared to water can be attributed to the higher moisture content of ethanol which caused further plasticization and degradation in both composites. It is worth mentioning that the reduction in stiffness observed for the water-immersed CFRP and CFRP/GNPs composites after impact at 5 and 10 J was similar, while for the samples immersed in ethanol, CFRP/GNPs stiffness showed lower reduction compared to CFRP samples after impact. The stiffness of CFRP/GNPs was reduced by 62% at 5 J and 65% at 10 J

compared to 72% and 70% for CFRP samples impacted at 5 and 10 J respectively. A reduction in flexural properties after immersion and impact was also reported by Korkees et al.[17] which was attributed to impact-induced damage and plasticization caused by the absorbed water.

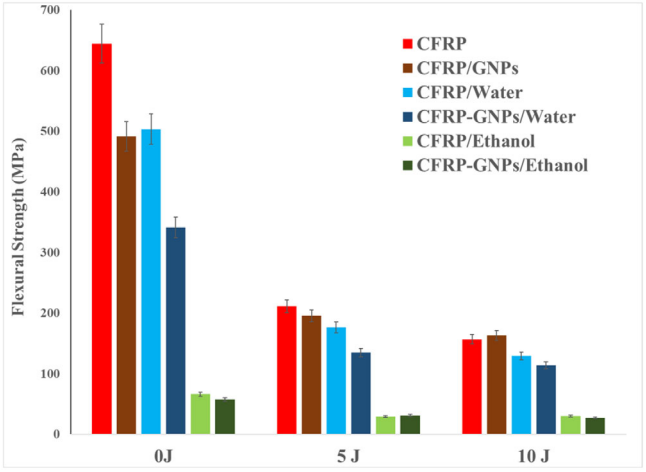

FIGURE 7 Flexural strength of samples before and after impact and immersion.

3.4 | Flexural strength

A similar trend to flexural modulus was observed for the flexural strength of CFRP after the GNPs addition, impact and immersion, Figure 7. The incorporation of NH_2 functionalized graphene was seen to reduce the strength of CFRP by 24%. This can be due to poor dispersion, agglomeration and bonding difficulty of GNPs in the matrix[43–45] rather than the theorized improvements in properties if good bonding and dispersion were achieved. Figure 7 also shows a large decrease in the flexural strength of both CFRP and CFRP/GNPs after a 5 J impact; a decrease of around 300 mPa is recorded for CFRP/GNPs while a decrease of around 450 mPa is recorded for CFRP. On the other hand, for the unconditioned samples impacted at 10 J, CFRP/GNPs composite lost around 330 mPa (67%) of its flexural strength while a reduction of 490 mPa (75%) of the flexural strength of the samples was observed for CFRP composites. This can be attributed to the increased toughness with the addition of GNPs as discussed before. However, these results show that once the samples have been impacted the flexural strength of CFRP and CFRP/GNPs become similar. This could indicate that CFRP/GNPs

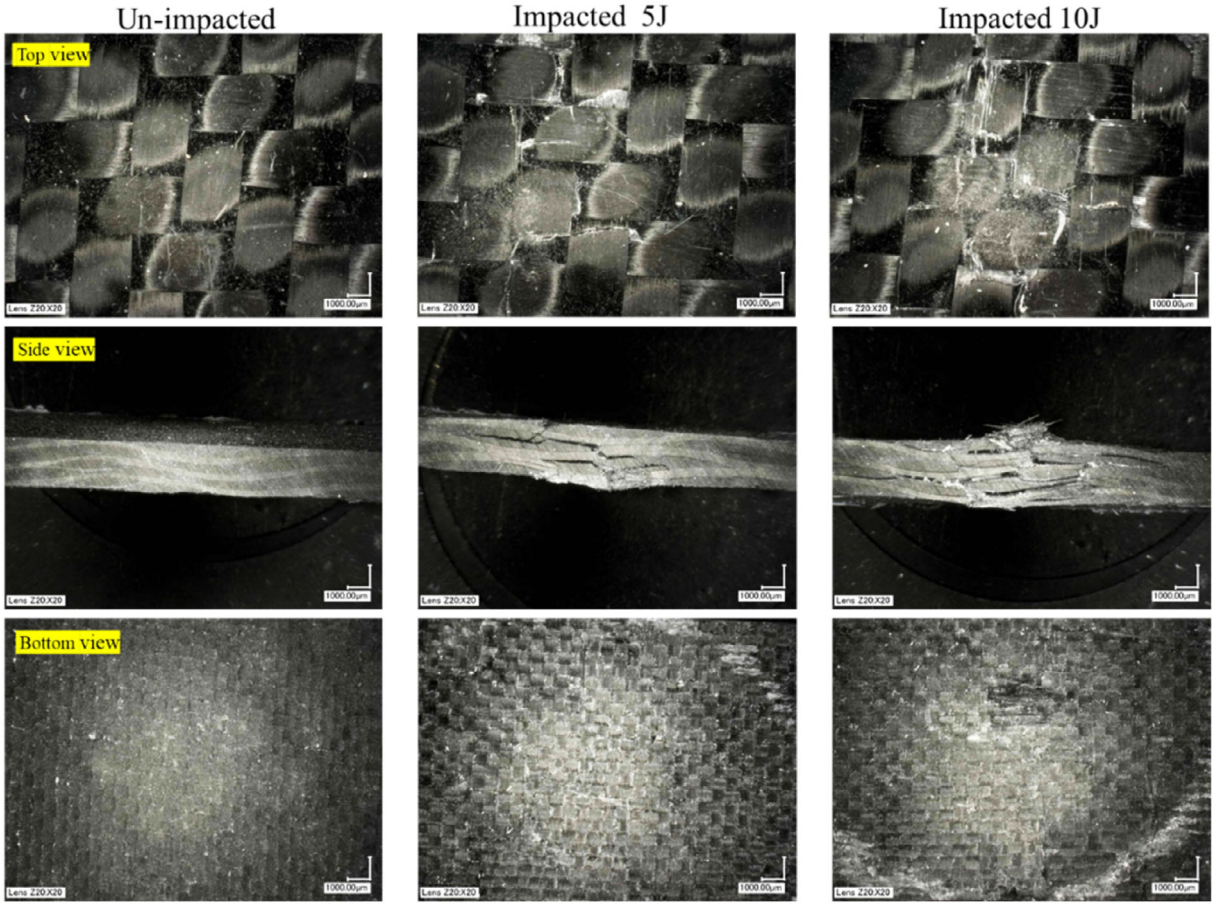

FIGURE 8 Optical microscopy images of carbon fiber reinforced polymer (CFRP) samples before and after impact.

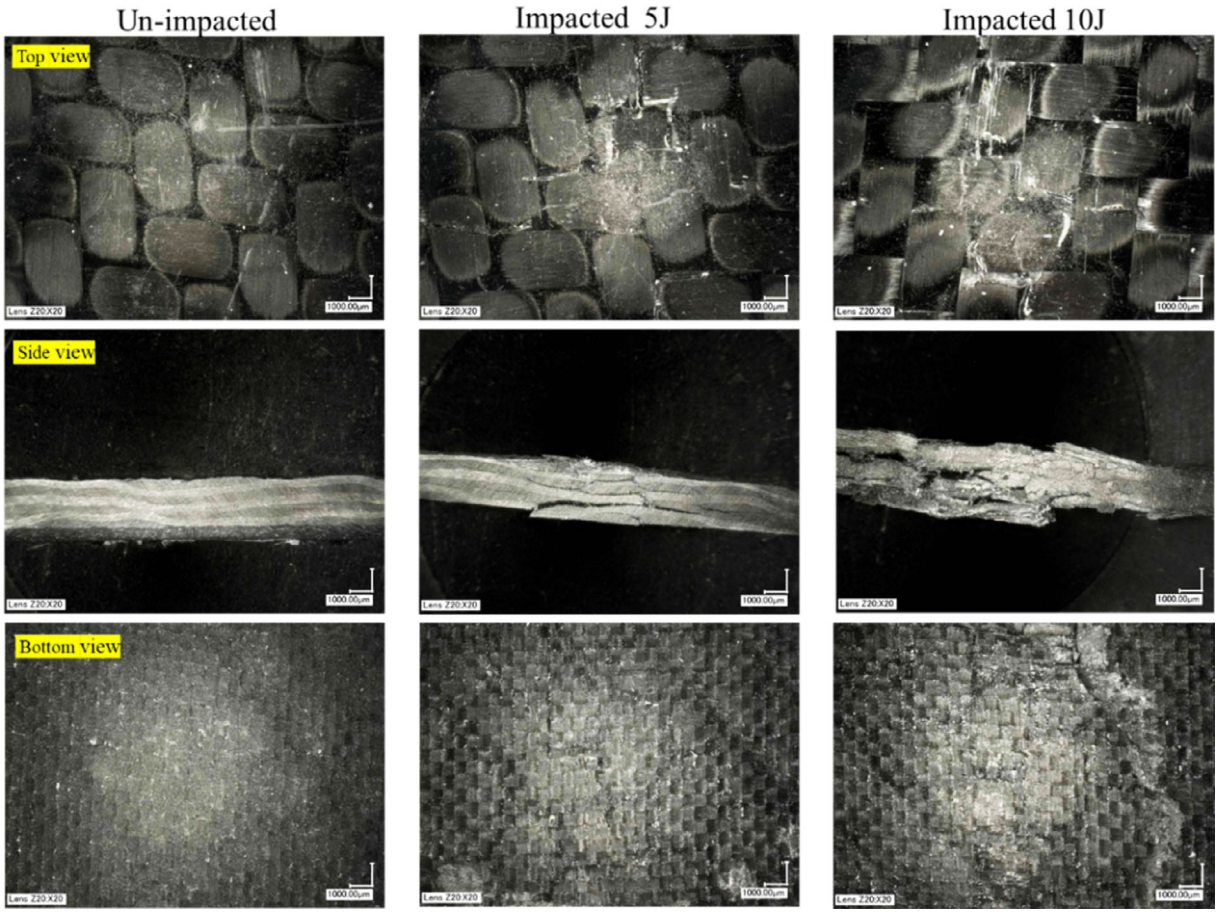

FIGURE 9 Optical microscopy images of carbon fiber reinforced polymer/graphene nanoparticles (CFRP/GNPs) samples before and after impact.

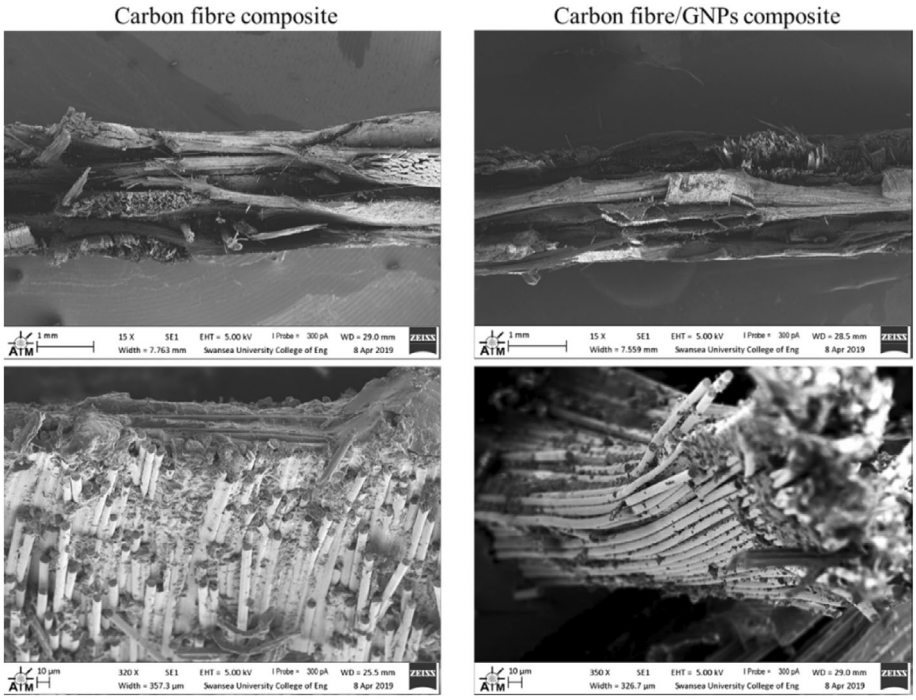

FIGURE 10 Scanning electron microscopy (SEM) images of the fracture surfaces after flexural test of carbon fiber reinforced polymer (CFRP) and CFRP/graphene nanoparticles (GNPs) samples.

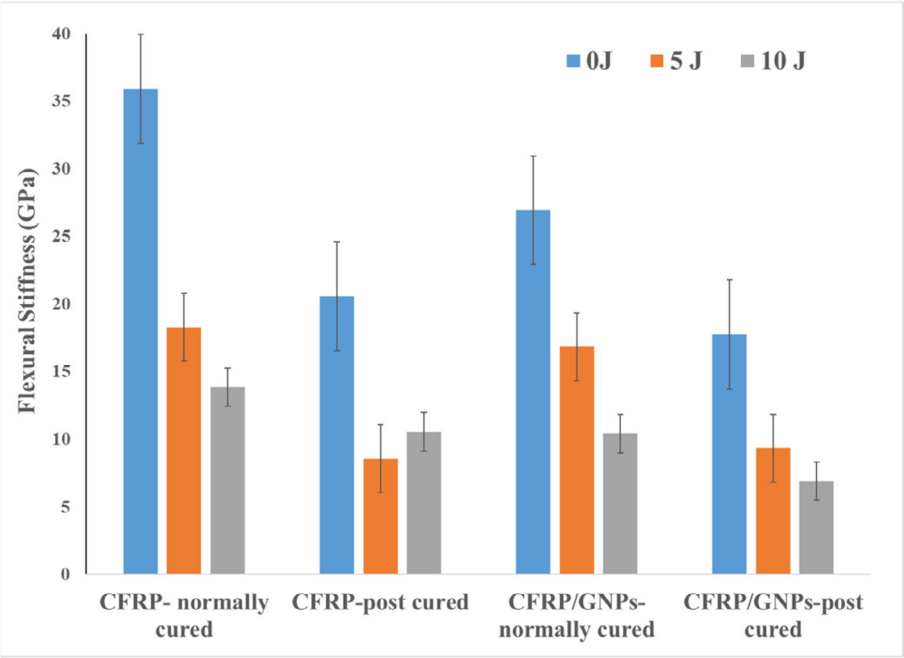

FIGURE 11 Flexural modulus of carbon fiber reinforced polymer (CFRP) and CFRP/graphene nanoparticles (GNPs) samples before and after post-curing.

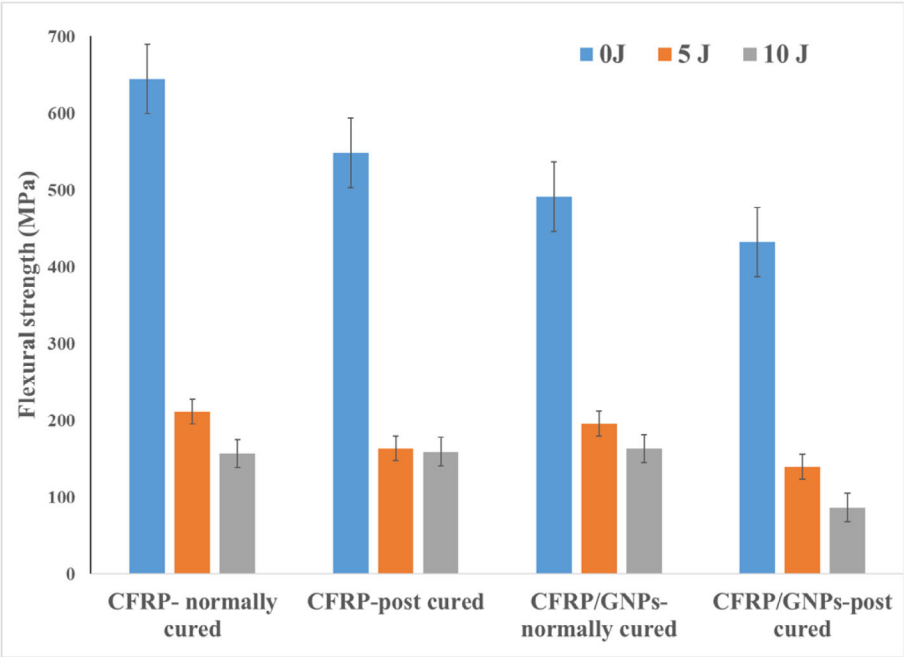

FIGURE 12 Flexural strength of carbon fiber reinforced polymer (CFRP) and CFRP/graphene nanoparticles (GNPs) samples before and after post-curing.

specimens have a higher toughness when compared to CFRP, but CFRP/GNP's much lower initial flexural strength finds that this increase in toughness provides no additional advantages in the flexural strength of the composite after impact. Based on the findings for the 3-point bend test CFRP/GNPs provides no advantages over CFRP. The effect of absorbed water on the flexural strength of CFRP and CFRP/GNPs is evident and the drop in strength of both composites is 22% and 31% respectively. On the contrary, a significant decrease in strength was observed in both composites by 89% after immersion in ethanol. Water-conditioned CFRP and CFRP/GNPs composites impacted at 5 J lost around 60% of their strength compared to unimpacted and conditioned samples, while around 70% reduction in strength was noted at 10 J. This is in good agreement with.[7,17,27] Similar behavior was observed for both composites after conditioning in ethanol and impacted at 5 and 10 J but with lower reductions of around 50% and 52% respectively. This is evident that increasing the impact energy increases the damage to the composites and also moisture uptake deteriorates the materials further.[17] Figure 7 illustrated that the effect of ethanol on the

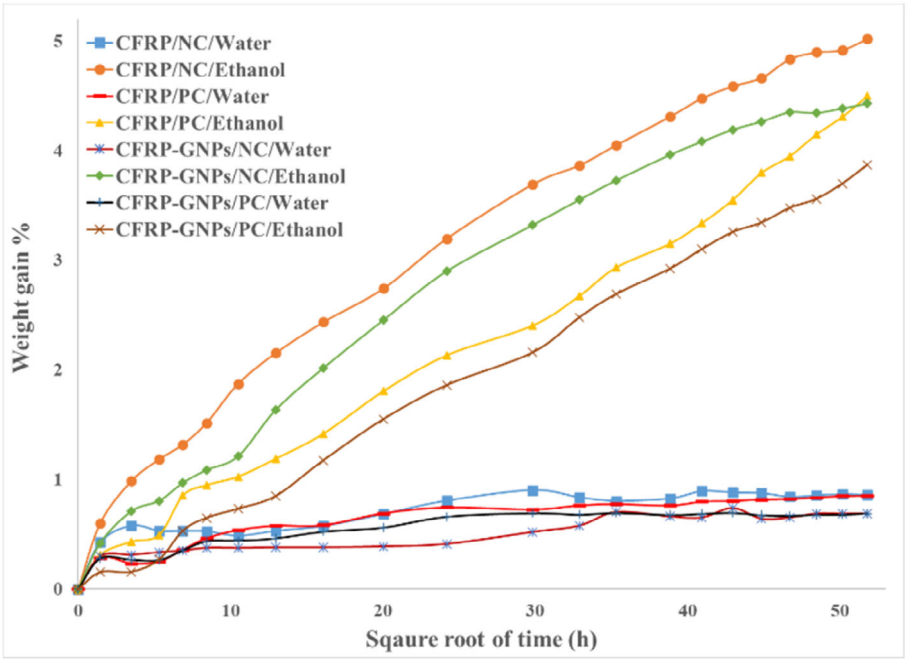

NC: Normally Cured. PC: Post Cured

FIGURE 13 Water and ethanol uptake of carbon fiber reinforced polymer (CFRP) and CFRP/graphene nanoparticles (GNPs) before and after post-curing. NC, normally cured; PC, post cured.

strength of both composites is immense compared to the effect of water where the materials lost around 80%–90% of their strength before and after impact. This is again due to the high content of ethanol in the composites compared to absorbed water which significantly plasticized and deteriorated the properties. This reduction in properties can be attributed to the high content of ethanol and the degradation of the epoxy in the presence of ethanol molecules.[19,58] This suggests that once a sample fractures, the process of epoxy degradation due to ethanol is almost complete at the sample saturation point.

3.5 | Failure modes of impacted CFRP and CFRP/GNPs

Samples were analyzed under a high depth of field microscope to compare failure modes between CFRP and CFRP/GNPs samples. The microscopy images of CFRP and CFRP/GNPs samples impacted at 5 and 10 J are shown in Figures 8 and 9. Both composites at both impact energies appear to have failed the same way by transverse cracks propagating through the layers and by delamination between the layers. This was found to be the dominant damage mode observed by other authors.[59] The level of damage severity is much higher at 10 J than 5 J which proves that the higher the impact energy the more damage the material experiences from an increase in crack propagation. The delamination and cracks formed in the CFRP/GNPs sample appear to be less severe than those found in the CFRP sample at 5 J impact energy, providing evidence that GNPs played a role in increasing the impact absorption capabilities and toughness. This justifies the similar reduction in strength and stiffness in CFRP/GNPs after impacted at 5 J to CFRP composite impacted at the same energy. Even though the damage at 10 J was more significant for CFRP/GNPs composite compared to CFRP composite, Figures 8 and 9 (side view), indicate that the impact damage caused momentous reduction for both composites in their flexural properties, but the CRFP/GNPs retained strength and stiffness quite similar to CFRP samples. This is also due to the role of GNPs which increased impact energy absorption and provided a toughening mechanism by enabling micro-crack deflection or crack pinning. Additionally, the size of impact areas of CFRP and CFRP/GNPs is seen to increase with an increase of impact energy, Figures 8 and 9 (top and bottom view).

After impact, due to the delamination and transverse cracks present in both composites, local instability is triggered, which ultimately reduces considerably their residual flexural strength and stiffness. SEM micrographs (Figure 8, top images) of the fracture surfaces after flexural testing shows both composites with and without GNPs. Various modes of failure were observed including delamination, fiber breakage, matrix cracking and fiber matrix interfacial debonding, Figure 9 (top images). The interfacial zone between carbon fibers and epoxy resin plays a vital role in transferring the stress from resin to reinforcement. This interfacial zone may also be considered as a specific element of the composite that could be affected by the addition of nanoparticles. The modification of the interface between

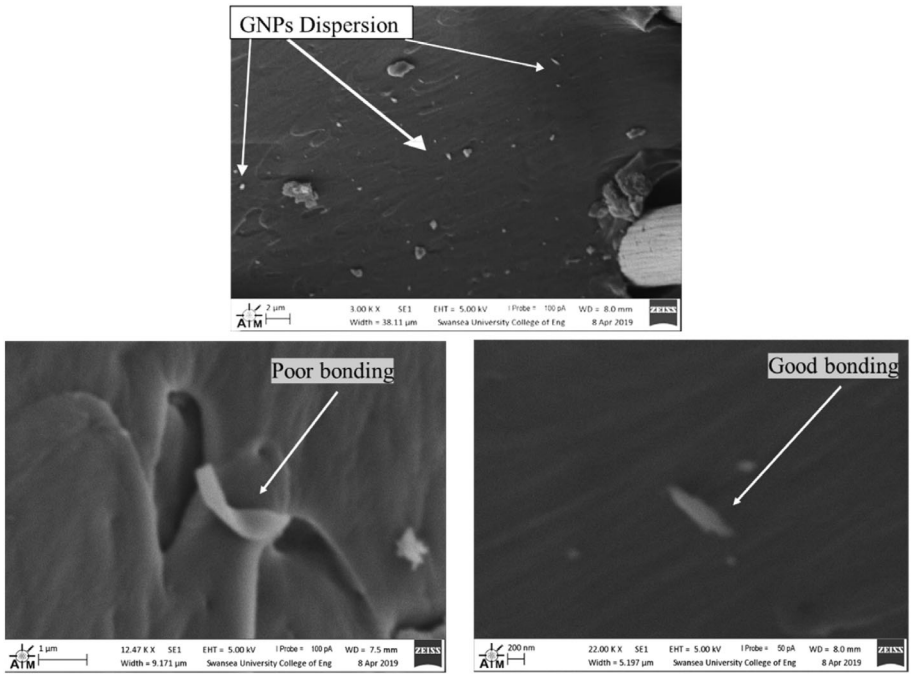

FIGURE 14 Scanning electron microscopy (SEM) images of dispersion and bonding of graphene nanoparticles.

fibers and resin by the addition of GNPs may explain the reduction of the flexural strength and stiffness of the CFRP/GNPs composite. To assess the quality of the interface, the fractured surfaces of both composites were inspected using SEM microscopy, Figure 10. CFRP samples showed greater matrix/fiber bonding with the epoxy resin still adhered to the fiber surfaces compared to CFRP/GNPs which showed significant matrix debonding consisting of clearer and smoother fiber surfaces.[60,61] Therefore, it can be said that the primary mode of failure in CFRP/GNPs is the failure at the interface which leads to fiber/matrix debonding and further upon loading results in the complete detachment of fibers from the matrix as shown in Figure 10. This is evident in the higher flexural properties of CFRP compared to CFRP/GNPs composites, as seen in Figures 6 and 7.

3.6 | Effects of post-curing on flexural and absorption properties

The temperature impact on the mechanical properties of fiber-reinforced composites during fabrication and operation can be significantly high. The curing of the epoxy resin controls the resulting cross-linking density, free volume, and glass transition temperature of the epoxy resin. The effect of curing and post-curing temperature on the properties and moisture absorption[62] of FRP during fabrication and the effect of various operating temperature conditions have already been studied. However, the post-curing effect on mechanical properties and moisture absorption on CFRP/GNPs composites is still not well investigated and further studies are needed. Kumar et al.[61] reported that the polymer matrix in FRP is not strong enough without post-curing, and the failure mode under loading is mostly due to the crushing of the polymer matrix. On the contrary, it has been found that post-curing can also lead to a reduction in the properties of composite materials due to the thermo-oxidation of the resin.[63] Therefore, three samples of CFRP/GNPs and three samples of CFRP were post-cured in an oven at 180°C for 2 h. This additional curing was carried out to study the effect of post-curing on the flexural properties of CFRP and CFRP/GNPs specimens before and after impact and also on the liquid absorption of these composites. Figures 11 and 12 showed that post-cured samples recorded slightly lower flexural properties compared to normally cured samples. This reduction might be because of thermal degradation or oxidative crosslinking within the epoxy polymer.[63]

Additionally, four cured samples each of CFRP and CFRP/GNPs were immersed in both ethanol and water to investigate if additional curing might improve uptake properties. Figure 13 shows the weight gain of CFRP and CFRP/GNPs samples immersed in water and ethanol before and after post-curing. It was found that additional curing had a slight effect on the uptake of water. Water uptake values appeared to closely follow a similar pattern as seen in normally cured samples. However, post-cured samples of both composites appeared to follow a more correct Fickian diffusion compared to normally cured samples, although both composites reached the same moisture content at saturation. This is because the

diffusivity constant is dependent on the hygrothermal aging temperature, whereas the moisture content at equilibrium is assumed to be an independent constant.[62]

On the contrary, for samples immersed in ethanol, up until the point where the research ended it appears that post-curing significantly slowed down the diffusion of ethanol in comparison to normally cured samples. Figure 13 illustrated that specimens that had been post-cured and immersed in ethanol had lower diffusion rates compared to normally cured samples. Although both composites attained seem to reach the same equilibrium moisture content irrespective of the aging temperature, the time taken to attain equilibrium moisture decreased significantly for post-cured samples. This might be due to the increased density of the cross-links in the composites and the reduction of the amount of unreacted OH groups in the post-cured samples.[62,63] When samples were post-cured, the number of OH group sites reduced, resulting in fewer ethanol molecules being absorbed.

3.7 | Evaluation of dispersion and bonding of GNPs in the composite

Good dispersion and bonding of graphene nanoparticles in the matrix is necessary to effectively utilize the properties of graphene throughout the polymer and thus enhancing the stress transfer between the matrix and the nanoparticles and the properties of the composite. Since the addition of NH_2 functionalized GNPs to CFRP composite decreased their flexural properties, an SEM characterization was conducted on the fracture surface to assess the microstructure. Visual proof of a good dispersion of graphene as seen in Figure 14 rules out the dispersion of graphene as a reason for the reduced flexural performance of CFRP/GNPs in comparison to CFRP. The good dispersion was reported by the authors in Jarrett and Korkees.[36] The functionalization of GNPs with amine functional groups allowed the breaking of the van der Waal forces between the nanoparticles that would otherwise lead to agglomeration and hence improving GNP immersion.[36,51] It also provides visual evidence that in terms of even distribution throughout the polymer, the manufacturing process using a twin screw extruder for compounding was effective. It is believed that this good dispersion of graphene is the reason that water uptake values for CFRP/GNPs samples were lower than for CFRP samples.

Furthermore, there was evidence of poor bonding of the graphene within the matrix, highlighted by the smooth GNP surface area, which was also reported by the authors Jarrett and Korkees[36] and can be seen in the microscopy images, in Figure 14. The clean and smooth surfaces of GNPs are an indication of a weak matrix/GNPs interaction which resulted in debonding leading to microcracking under load, propagation, and eventual failure.[36,64] Despite the poor bonding observed in most of the samples, a strong bonding was seen in some areas, Figure 14, which might be responsible for the increased toughness. This good bonding was reported by Korkees et al.[51] However, poor bonding is evident that the strong mechanical properties of graphene were not used effectively within this composite and hence the lower flexural values of CFRP/GNPs in comparison to CFRP were obtained. This is in good agreement with Jarrett and Korkees[36] and Wang et al.[64] where a decrease in mechanical properties was observed for the same reason. If better bonding was achieved, CFRP/GNPs could provide better flexural strength in comparison to CFRPs.[65]

4 | CONCLUSION

This study investigated the flexural performance of carbon fiber composites modified with 2 wt% NH_2-GNPs under liquid absorption and low energy impact. In comparison to the reference CFRP material, the GNPs/CFRP samples did not show any improvement in tensile strength or flexural strength before or after immersion and impact. However, an improvement in the resistance to moisture diffusion was observed with the addition of the 2 wt% NH_2-GNPs into the CFRP samples. The incorporation of NH_2-GNPs in the epoxy matrix of CFRP decreased the flexural modulus and the strength of the composites by 25% and 24%, respectively. A limitation with the dispersion, agglomeration and bonding difficulty between the GNPs dispersed within the epoxy is to be the reason behind the reduction in flexural properties. Further reduction of between 30% and 70% was observed in both composites after moisture absorption and impact which can be attributed to matrix plasticization and damages caused by the low energy impact in addition to the dispersion and bonding limitations of GNPs. CFRP/GNPs samples were found to have consistently lower diffusion rates and water maximum contents of both water and ethanol compared to CFRP. A reduction of 0.2% and 0.5% was observed in the weight gain of CFRP/GNPs samples compared to CFRPs in water and ethanol, respectively. However, Ethanol content at saturation (4.5%) was much higher compared to water content (0.6%) for CFRP/GNPs samples and similar behavior was noticed for CFRP samples. This was found to cause large degradation of both CFRP and CFRP/GNPs resulting in a large decline in the samples' flexural properties. On the other hand, the maximum reduction in diffusion rate occurred at 5 J impact for ethanol immersion by 46.4%, and 10 J impact for

water immersion, by 44.8%. High-depth of field imaging found similar failure modes for CFRP and CFRP/GNPs. It was also found that as impact energy increased, so did the severity of failure and size of the impact area. Impact damage was seen to be less in CFRP/GNPs samples in comparison to CFRP, indicating higher toughness. SEM images found there was a good dispersion of graphene within the CFRP/GNPs samples, but found that graphene bonding was mostly poor, which could be the main factor in the reduction of the CFRP/GNPs' flexural properties in comparison to CFRP.

Additional research into the effects of post-curing found that the flexural properties of both composites decreased after post-curing at 180°C. However, a slight reduction in water absorption was observed after post-curing compared to the more significant decrease observed with ethanol absorption. Furthermore, slower diffusion was recorded for the post-cured samples of both composites compared to the normally cured samples. This was mainly due to the increase in the cross-link density and the reduction of unreacted OH groups in the post-cured composites.

This is an ongoing study, and these early-stage results did not achieve what was expected in terms of the potential of GNPs to improve the flexural properties of carbon fiber/epoxy composites but provided evidence for the ability of graphene nanoparticles to hinder moisture absorption and reduce diffusion rate into carbon fiber/epoxy composites. This is a hugely beneficial characteristic in most real-world engineering applications of CFRP. Further investigation into the manufacturing method and the use of different GNPs functionalization and loadings is required to improve dispersion and bonding between the GNPs and the epoxy resin in the composite.

ACKNOWLEDGMENTS

This research did not receive specific grants from funding agencies in the public, commercial, or not-for-profit sectors.

DATA AVAILABILITY STATEMENT

The raw/processed data required to reproduce these findings cannot be shared at this time as the data also forms part of an ongoing study.

ORCID

Feras Korkees https://orcid.org/0000-0002-5131-6027
Russo Swart https://orcid.org/0000-0001-6521-7479

REFERENCES

[1] S. K. Sardiwal, B. V. Sai Anoop, G. Susmita, L. Vooturi, S. A. Uddin, *Glob. J. Res. Eng. D Chem. Eng* **2014**, *14*, 5.
[2] M. Maria, *INCAS Bull.* **2013**, *5*, 139.
[3] A. J. Timmis, A. Hodzic, L. Koh, M. Bonner, C. Soutis, A. W. Schäfer, L. Dray, *Int. J. Life Cycle Assess* **2015**, *20*, 233.
[4] C. Bonavolontà, M. Valentino, G. Peluso, A. Barone, *IEEE Trans. Appl. Supercond* **2007**, *17*, 772.
[5] B. Yang, Y. Huang, L. Cheng, *Infrared Phys. Technol.* **2013**, *60*, 166.
[6] F. L. Matthews, R. D. Rawlings, *Composite Materials: Engineering and Science*, Chapman and Hall, London, UK **1994**.
[7] Y. Aoki, K. Yamada, T. Ishikawa, *Compos. Sci. Tech.* **2008**, *68*, 1376.
[8] M. O. W. Richardson, M. J. Wisheart, *Compos. Part A: Appl. Sci. Manuf.* **1996**, *27*, 1123.
[9] M. D. Freitas, A. Silva, L. Reis, *Compos. B: Eng.* **2000**, *31*, 199.
[10] F. Caputo, A. De Luca, G. Lamanna, V. Lopresto, A. Riccio, *Compos. B: Eng.* **2015**, *68*, 385.
[11] E. Greenhalgh, S. Singh, D. Roberts. presented at *Proc. ICCM–11*, Gold Coast, Australia, 14-18 July **1997**.
[12] Y. I. Tsai, E. J. Bosze, E. Barjasteh, S. R. Nutt, *Compos. Sci. Tech.* **2009**, *69*, 432.
[13] G. M. Candido, M. L. Costa, S. F. M. de Almeida, M. C. Rezende, *Compos. B: Eng.* **2008**, *39*, 490.
[14] S. B. Kumar, I. Sridhar, S. Sivashanker, *Mater. Sci. Eng. Part A* **2008**, *498*, 174.
[15] A. P. Cysne Barbosa, A. P. Ana, E. S. S. Guerra, F. K. Arakaki, M. Tosatto, M. C. Maria, J. D. José, *Compos. B: Eng.* **2017**, *110*, 298.
[16] J. C. Arnold, S. Alston, F. Korkees, S. Dauhoo, R. Adams, R. Older. presented at *Innov. Compos.: Compos.*, UK 10th Annual Conference 5-6 May **2010**.
[17] F. Korkees, C. Arnold, S. Alston, *Polym. Compos.* **2018**, *39*, 2771.
[18] F. Korkees, S. Alston, C. Arnold, *Polym. Compos.* **2018**, *39*, 2305.
[19] F. Korkees, R. Swart, I. Barsoum, *Polym. Eng. Sci* **2022**, *62*, 1582.
[20] F. Korkees, C. Arnold, S. Alston, *Polym. Eng. Sci* **2018**, *58*, 2175.
[21] X. Qian, Y. G. Zhang, X. F. Wang, Y. J. Heng, J. H. Zhi, *Surf. Interface Anal.* **2016**, *48*, 1271.
[22] J. C. Arnold, S. M. Alston, F. Korkees, *Compos. Part A: Appl. Sci. Manuf.* **2013**, *55*, 120.
[23] J. C. Arnold, F. Korkees, S. M. Alston. presented at *ECCM15—15th Eur. Conf. Compos. Mater.*, Venice, Italy, 24-28 June **2012**.
[24] F. Korkees, S. M. Alston, J. C. Arnold. presented at *20th Int. Conf. Compos. Mater.*, Copenhagen, 19-24th. **2015**.
[25] S. M. Alston, J. C. Alston, F. Korkees. presented at *ECCM15—15th Eur. Conf. Compos. Mater.*, Venice, Italy, 24-28 June **2012**.
[26] F. Korkees. *PhD Thesis*, Swansea University (UK) **2012**.
[27] K. Imielinska, L. Guillaumat, *Compos. Sci. Tech* **2004**, *64*, 2271.
[28] S. Meguid, Y. Sun, *Mater. Des.* **2004**, *25*, 289.
[29] C. Deepa, L. Rajeshkumar, M. Ramesh, *J. Mater. Res. Technol.* **2022**, *19*, 2657.
[30] M. Ramesh, L. Rajeshkumar, R. Bhoopathi, *Carbon Lett.* **2021**, *31*, 557.
[31] K. S. Novoselov, V. I. Fal'Ko, L. Colombo, P. R. Gellert, M. G. Schwab, K. Kim, *Nature* **2012**, *490*, 192.
[32] T. Ramanathan, A. A. Abdala, S. Stankovich, D. A. Dikin, M. Herrera-Alonso, R. D. Piner, D. H. Adamson, H. C. Schniepp, X. Chen, R. S. Ruoff, S. T. Nguyen, I. A. Aksay, R. K. Prud'Homme, L. C. Brinson, *Nat. Nanotechnol.* **2008**, *3*, 327.

[33] G. Lin, G. Xie, G. Sui, R. Yang, *Compos. B: Eng.* **2012**, *43*, 44.
[34] M. H. Woldemarium, G. Belingardi, E. G. Koricho, D. T. Reda, *AIMS Mater. Sci.* **2019**, *6*, 1191.
[35] M. Ekramul Islam, T. H. Mahdi, M. V. Hosur, S. Jeelani, *Proc. Eng.* **2015**, *105*, 821.
[36] W. Jarrett, F. Korkees, *Polymer* **2022**, *252*, 124921.
[37] J. B. Knoll, B. T. Riecken, N. Kosmann, S. Chandrasekaran, K. Schulte, B. Fiedler, *Compos. Part A: Appl. Sci. Manuf.* **2014**, *67*, 233.
[38] M. Abu-Okail, N. A. Alsaleh, W. M. Farouk, A. Elsheikh, A. Abu-Oqail, Y. A. Abdelraouf, M. A. Ghafaar, *J. Mater. Res. Technol.* **2021**, *14*, 2624.
[39] H. R. Pakravan, H. Yari, *Polym. Adv. Technol.* **2018**, *29*, 970.
[40] S. Sivasaravanan, V. K. Bupesh, V. Sathvik, S. D. Reddy, *J. Chem. Tech. Res.* **2016**, *9*, 189.
[41] M. H. Gabr, W. Okumura, H. Ueda, W. Kuriyama, K. Uzawa, I. Kimpara, *Compos. B: Eng.* **2015**, *69*, 94.
[42] E. G. Koricho, A. Khomenko, M. Haq, L. T. Drzal, G. Belingardi, B. Martorana, *Compos. Struct.* **2015**, *134*, 789.
[43] G. Watson, K. Starost, P. Bari, N. Faisal, S. Mishra, J. Njuguna, *IOP Conf. Ser.: Mater. Sci. Eng.* **2017**, *195*, 012009.
[44] D. L. Zhao, R. H. Qiao, C. Z. Wang, Z. M. Shen. presented at *Proc. Asian Int. Conf. Adv. Mater.* (*AICAM 2005*), Beijing, China, 3-5 November **2006**, p. 517.
[45] Y. Zare, K. P. Rhee, D. Hui, *Compos. B: Eng.* **2017**, *122*, 41.
[46] O. Starkova, S. Gaidukovs, O. Platnieks, A. Barkane, K. Garkusina, E. Palitis, L. Grase, *Polym. Degrad. Stab.* **2021**, *191*, 109670.
[47] S. G. Prolongo, A. Jiménez-Suárez, R. Moriche, A. Ureña, *Appl. Sci.* **2018**, *8*, 1550.
[48] D. Cai, M. Song, *J. Mater. Chem.* **2010**, *20*, 7906.
[49] M. S. Senthil Kumar, N. M. S. Raju, P. S. Sampath, L. S. Jayakumari, *Rev. Adv. Mater. Sci.* **2014**, *38*, 40.
[50] Y. Tian, H. Zhang, Z. Zhang, *Compos. Part A: Appl. Sci. Manuf.* **2017**, *98*, 1.
[51] F. Korkees, A. Aldrees, I. Barsoum, D. Alshammari, *J. Compos. Mater.* **2021**, *55*, 2211.
[52] T. Ramanathan, H. Liu, L. C. Brinson, *J. Polym. Sci. Part B* **2006**, *44*, 470.
[53] D. Cho, S. Lee, G. Yang, H. Fukushima, L. T. Drzal, *Mater. Eng.* **2005**, *290*, 179.
[54] C. H. Shen, G. S. Springer, *J. Compos. Mater.* **1976**, *10*, 2.
[55] V. O. Startsev, S. V. Panin, O. V. Startsev, *Mech. Compos. Mater.* **2016**, *51*, 761.
[56] H. Sharma, A. Kumar, S. Rana, L. Guadagno, *Polymer* **2022**, *14*, 1548.
[57] Y. J. Weitsman, Y. J. Guo, *Compos. Sci. Technol* **2002**, *62*, 889.
[58] J. Tiihonen, I. Markkanen, A. Kärki, P. Äänismaa, M. Laatikainen, E. Paatero, *Chem. Eng. Sci.* **2002**, *57*, 1885.
[59] M. Aktas, C. Atas, B. M. İçten, R. Karakuzu, *Compos. Struct.* **2009**, *87*, 307.
[60] D. A. Hernandez, C. A. Soufen, M. O. Orlandi, *Mater. Res* **2017**, *20*, 951.
[61] D. S. Kumar, M. J. Shukla, K. K. Mahato, D. K. Rathore, R. K. Prusty, B. C. Ray, *Mater. Sci. Eng.* **2015**, *75*, 1.
[62] A. N. Rajaram, C. G. Boay, N. Srikanth, *Comput. Commun.* **2020**, *22*, 100507.
[63] C. Campana, R. Léger, R. Sonnier, L. Ferry, P. Ienny, *Compos. Part A: Appl. Sci. Manuf.* **2018**, *107*, 171.
[64] F. Wang, L. T. Drzal, Y. Qin, Z. Huang, *J. Mater. Sci.* **2015**, *50*, 1082.
[65] A. K. Srivastava, V. Gupta, C. S. Yerramalli, A. Singh, *Compos. B: Eng.* **2019**, *179*, 107539.

How to cite this article: F. Korkees, E. Morris, W. Jarrett, R. Swart, *Polym. Compos.* **2023**, *44*(6), 3325. https://doi.org/10.1002/pc.27324